

Competition between Bose-Einstein Condensation and Spin Dynamics

B. Naylor,^{1,2} M. Brewczyk,³ M. Gajda,⁴ O. Gorceix,^{1,2} E. Maréchal,^{1,2} L. Vernac,^{1,2} and B. Laburthe-Tolra^{1,2}

¹Université Paris 13, Sorbonne Paris Cité, Laboratoire de Physique des Lasers, F-93430 Villetaneuse, France

²CNRS, UMR 7538, LPL, F-93430 Villetaneuse, France

³Wydział Fizyki, Uniwersytet w Białymstoku, ul. K. Ciołkowskiego 1L, PL-15-245 Białystok, Poland

⁴Institute of Physics, Polish Academy of Sciences, Aleja Lotników 32/46, PL-02668 Warsaw, Poland

(Received 6 July 2016; published 27 October 2016)

We study the impact of spin-exchange collisions on the dynamics of Bose-Einstein condensation by rapidly cooling a chromium multicomponent Bose gas. Despite relatively strong spin-dependent interactions, the critical temperature for Bose-Einstein condensation is reached before the spin degrees of freedom fully thermalize. The increase in density due to Bose-Einstein condensation then triggers spin dynamics, hampering the formation of condensates in spin-excited states. Small metastable spinor condensates are, nevertheless, produced, and they manifest in strong spin fluctuations.

DOI: 10.1103/PhysRevLett.117.185302

Dilute quantum gases are especially suited for the investigation of nonequilibrium dynamics in closed or open quantum systems, for example, associated with the physics of thermalization [1], prethermalization [2], or localization [3]. In particular, they provide a platform to study the kinetics of Bose-Einstein condensation. Soon after the first Bose-Einstein condensates (BECs) were obtained, it was possible to, for example, investigate how the BEC nucleates [4,5]. More recently, experiments performing a temperature quench below the superfluid transition investigated the dynamics of spontaneous symmetry breaking [6] and revealed the production of long-lived topological defects [7]. The aim of this Letter is to extend the dynamical studies of Bose-Einstein condensation to the case of a multicomponent Bose gas, in order to establish the mechanisms to reach both superfluid and magnetic orders. While these orders are intrinsically connected due to Bose stimulation [8,9] (which contrasts with the case of Fermi fluids [10]), it was predicted that strong spin-dependent interactions induce spin ordering at a finite temperature *above* the BEC transition [11].

We find that the dynamics of Bose-Einstein condensation in our experiment is drastically modified due to spin-changing collisions arising from relatively strong spin-dependent interactions. Thermalization of the spin degrees of freedom is influenced by the occurrence of a BEC and, in turn, influences which multicomponent BECs can be produced. Our experiment also demonstrates the difficulty of thermalizing the spin degrees of freedom, which has a strong impact on the spin distribution of the BECs, and on their lifetime. This is of particular relevance for large spin atoms, and most notably for strongly magnetic atoms such as Cr [12,13], Er [14], and Dy [15] for which dipolar relaxation strongly limits the lifetime of multicomponent gases [16].

We induce fast evaporative cooling of a multicomponent $s = 3$ chromium thermal cloud by lowering the depth of a

spin-insensitive optical dipole trap (ODT) [see Fig. 1(a)]. When the gas is only slightly depolarized, the thermal gas of the most populated, lowest energy state, $m_s = -3$, rapidly saturates (i.e., it reaches the maximal number of atoms in motional excited states allowed by Bose statistics [17]) and a BEC is produced for this spin state. Saturation is also reached for the thermal gas in the second-to-lowest energy state, $m_s = -2$. However, surprisingly, this state fails to condense and the BEC remains fully magnetized. In contrast, when the experiment is performed with an initially more depolarized thermal gas, spinor (i.e., multicomponent) condensates are

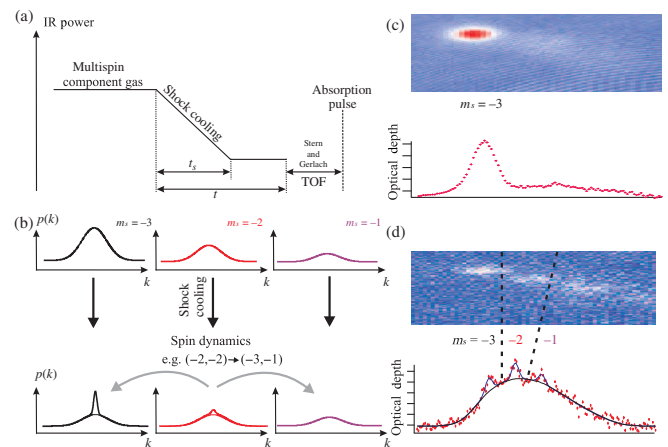


FIG. 1. (a) Experimental sequence showing the reduction in the ODT intensity in a duration t_s . An absorption image is taken after a time t and Stern-Gerlach separation. (b) Simple sketch of the evolution of the momentum distributions [$p(k)$] of atoms in the three lowest spin-excited states, illustrating the difficulty of achieving a BEC (a peak on top of the broad thermal k distribution) in spin-excited states due to spin dynamics. Absorption pictures showing (c) a BEC in $m_s = -3$, and a thermal gas in other spin states for a gas initially prepared with magnetization $M = -2.5 \pm 0.25$, and (d) a small multicomponent BEC for $M = -2.00 \pm 0.25$.

obtained, although they remain very small [see Fig. 1(d)] and show strong spin fluctuations. Comparison with numerical simulations based on the classical field approximation (CFA) [18] reveals that the difficulty in obtaining a multicomponent BEC is due to spin-exchange collisions, which rapidly empty the condensates in spin-excited states by populating spin states for which the thermal gas is not yet saturated. There is an intriguing interplay between condensation and spin dynamics, as the large increase in density associated with BEC triggers fast spin dynamics, which, in turn, tends to deplete the BEC in spin-excited states. The observed spin fluctuations in the BEC are ascribed to a combined effect of phase fluctuations due to symmetry breaking at the BEC transition and spin dynamics.

To prepare an incoherent spin mixture of thermal gases, we start with a thermal gas of 2×10^4 ^{52}Cr atoms, at $T = 1.1 \times T_c = 440 \pm 20$ nK, polarized in the Zeeman state $m_s = -3$. We adiabatically reduce the magnetic field B to 1.5 ± 0.2 mG so that the Zeeman energy is of the same order as the thermal kinetic energy. Depolarization of the cloud is driven by magnetization-changing collisions associated with dipole-dipole interactions [19–21]. We obtain a gas having a longitudinal magnetization $M = -2.50 \pm 0.25$, with $M \equiv \sum_{i=-s}^s i n_i$ (n_i is the relative population in the Zeeman state $m_s = i$). We then reduce the trap depth by applying an approximately linear ramp to the ODT laser intensity in a time t_S . The trap frequencies are then reduced from (400, 325, 285) Hz to (230, 190, 160) Hz. This procedure results in fast forced evaporative cooling of all Zeeman states [which we refer to as “shock cooling”; see Fig. 1(a)]. We study spin dynamics and condensation dynamics by measuring both the spin and momentum distributions as a function of the time t after the beginning of the evaporation ramp. This measurement is performed by switching off all of the trapping lights and applying an average magnetic field gradient of $3.5 \text{ G} \cdot \text{cm}^{-1}$ during a 6 ms time of flight to perform a Stern-Gerlach separation of the free-falling atoms.

Figure 1(c) shows a typical absorption picture. It reveals a BEC in $m_s = -3$ and a thermal gas in spin-excited states. We extract the number of thermal and condensed atoms of each spin state through bimodal fits accounting for Bose statistics. We plot in Fig. 2 the thermal atom numbers as well as the condensate fractions in $m_s = (-3, -2)$ as a function of time t for a shock cooling time $t_S = 500$ ms. We found similar results for $t_S = 250$ ms and $t_S = 1$ s.

The gray area in Fig. 2 highlights a relatively long cooling time during which the $m_s = -3$ and $m_s = -2$ gases hold approximately the same number of thermal atoms, and there is a BEC in the lowest state, $m_s = -3$, but not in $m_s = -2$. This phenomenon is surprising because it shows that the $m_s = -2$ component fails to undergo Bose-Einstein condensation even though its thermal gas is saturated. Indeed, $m_s = -2$ and $m_s = -3$ thermal atoms have the same measured mechanical temperature (within

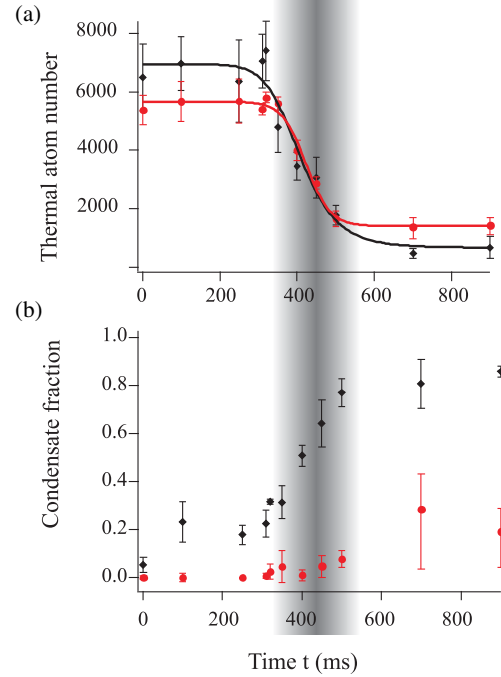


FIG. 2. (a) Number of thermal atoms in $m_s = -3$ (the black diamonds) and $m_s = -2$ (the red disks) as a function of time t for a shock cooling time $t_S = 500$ ms. (b) Corresponding condensate fractions in $m_s = -3$ (the black diamonds) and $m_s = -2$ (the red disks). The shaded region highlights when both $m_s = -3$ and $m_s = -2$ thermal clouds are saturated, but only $m_s = -3$ atoms condense.

our 5% experimental uncertainty), experience the same trapping potential, and both interact through the $S = 6$ molecular potential with the existing $m_s = -3$ BEC. Therefore, the $m_s = -2$ cloud has the same thermodynamical properties as the $m_s = -3$ thermal gas and, similar to the latter spin component, should condense for further cooling [17]. However, a BEC does not occur in this state until $t \leq 700$ ms. Only for $t \geq 700$ ms do we also distinguish a very small BEC in $m_s = -2$. This demonstrates that a BEC in $m_s = -2$ hardly forms, although the thermal gas is saturated and cooling proceeds.

To interpret these observations, we stress that magnetization-changing collisions occur on a larger time scale than shock cooling dynamics and can be neglected, contrary to Refs. [19,21]. Here, spin dynamics is almost entirely controlled by spin-exchange interactions at constant magnetization driven by spin-dependent contact interactions [9]. A key point is that, for an incoherent mixture, the spin dynamics rate $\gamma_{i,j}^{k,l}$ for the spin-changing collision ($m_s = i, m_s = j \rightarrow m_s = k, m_s = l$) is set by the density of the cloud through $\gamma_{i,j}^{k,l} = n \sigma_{i,j}^{k,l} v$, with n being the atomic density, v the average relative atomic velocity, and $\sigma_{i,j}^{k,l}$ the relevant cross section within the Born approximation [22]. This rate is extremely sensitive to the presence of a BEC (which enhances n). Therefore, the emergence of a BEC in

a spin-excited state should trigger faster spin dynamics. In addition to these incoherent spin-exchange processes, a BEC can also trigger coherent spin oscillations due to forward scattering, with a typical rate $\Gamma_{i,j}^{k,l} = (4\pi\hbar/m)n\sum_S a_S \langle i, j|S\rangle \langle S|k, l\rangle$, where the sum is on even molecular potentials S , with an associated scattering length a_S . Our interpretation for the absence of a BEC in the state $m_s = -2$ is thus that a large BEC cannot form in this state because fast spin-exchange processes $(-2, -2) \rightarrow (-1, -3)$ deplete the BEC as soon as it is produced. Thus, spin dynamics and condensation dynamics are strongly intertwined.

To check out this interpretation, we have performed numerical simulations using the Gross-Pitaevskii (GP) equation and the classical field approximation to describe thermal states. According to the CFA, the GP equation determines the evolution of the classical field which is a complex function carrying the information on both the condensed and thermal atoms [18,23,24]. The initial classical field corresponds to 13×10^3 Cr atoms at the critical temperature of about 400 nK and with the experimental Zeeman distribution. To describe such a sample, we follow the prescription given in Ref. [24]. We start with the Maxwell-Boltzmann density corresponding to the chosen number of atoms, the temperature, and the trapping potential. The classical field is built from this density by, first, multiplying its square root by a phase factor and, second, by disturbing the phase in space to pump in enough kinetic energy to satisfy the equipartition law. Evaporative cooling is mimicked by adding a purely imaginary potential to the GP equation at the edge of the numerical grid. Our simulations use the same trap geometry as the experimental one and, more specifically, the same time-dependent trap frequencies.

Our simulations confirm the existence of a saturated $m_s = -2$ gas with almost no condensed atoms in this state (see Fig. 3). To evaluate the impact of spin-exchange processes on the dynamics of condensation, we have reproduced these simulations while assuming $a_4 = a_6$. In this case, the rates associated with the spin-exchange processes $(-2, -2) \rightarrow (-1, -3)$, $\gamma_{-2,-2}^{-1,-3}$ and $\Gamma_{-2,-2}^{-1,-3}$ —which scale, respectively, as $(a_6 - a_4)^2$ and $(a_6 - a_4)$ —both vanish. As shown in Fig. 3, a much larger BEC then forms in the spin-excited state $m_s = -2$. This confirms the crucial role of spin-dependent contact interactions in the dynamics of Bose-Einstein condensation. On the other hand, our numerical simulations show that dipole-dipole interactions play a negligible role, except when the magnetic field is well below 1 mG (and, therefore, well below the experimental situation).

It is interesting to face our observations with the accepted scenario for the thermodynamics of noninteracting multi-component Bose gases at fixed magnetization [25]. In this picture, a BEC polarized in the most populated state forms below a first critical temperature; all of the other thermal spin states saturate *simultaneously* and condense below a

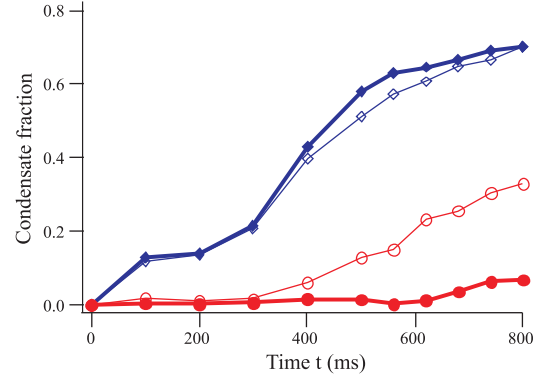


FIG. 3. Numerical results. Evolution of the condensate fractions for different values of a_4 (blue diamonds, $m_s = -3$; red circles, $m_s = -2$). Filled markers correspond to the experimental case: $a_4 = 64a_B$ and $a_6 = 102.5a_B$ [16], where a_B is the Bohr radius. Empty markers correspond to simulations where a_4 is set equal to a_6 to suppress spin dynamics. A significant BEC fraction in $m_s = -2$ is then obtained.

second critical temperature [25]. In our situation, our observations indicate that the external degrees of freedom have reached an equilibrium, at an effective temperature which we find to be identical for all spin components. However, although the thermal clouds of the two lowest spin components are saturated, the other thermal clouds are not saturated. This difference, compared to the prediction of Bose thermodynamics at equilibrium, shows that the spin degrees of freedom in our experiment remain out of equilibrium.

This lack of thermal equilibrium for the spin degrees of freedom results from the fact that spin-exchange processes for the thermal gas are slow in regards to condensation dynamics. For example, the rate of the dominant spin-exchange term, averaged over density, $\gamma_1 = (n_0\sigma_{-2,-2}^{-1,-3}v/2\sqrt{2})$, with n_0 being the peak atomic density, is typically 3 s^{-1} for a thermal gas at T_C . A much longer time t_S would therefore be necessary in order to reach spin equilibrium. This rate is slow compared to typical thermalization rates of the mechanical degrees of freedom, e.g., $\gamma_2 = (n_0\sigma_{-2,-2}^{-2,-2}v/2\sqrt{2}) \approx 40 \text{ s}^{-1}$. $\gamma_2 \gg \gamma_1$ insures that the mechanical degrees of freedom thermalize faster than the spin degrees of freedom, and that a small $m_s = -2$ BEC can, in principle, be formed. However, once the $m_s = -2$ BEC is formed, the rates associated with the $(-2, -2) \rightarrow (-3, -1)$ collisions rise to, typically, $\gamma_{1,\text{BEC}} \approx 7 \text{ s}^{-1}$ and $\Gamma_{-2,-2}^{-1,-3} \approx 60 \text{ s}^{-1}$ (for 500 atoms in the condensate). Spin-exchange collisions then deplete the $m_s = -2$ BEC as fast as it is created and a multicomponent BEC cannot be sustained due to the lack of saturation of the $m_s = -1$ thermal gas.

Under our experimental conditions, nonsaturated spin-excited states thus act as a reservoir into which population may be dumped, thus preventing a BEC but in the stretched state, which is the only collisionnally stable one. The

situation bears some analogy to the condensation of magnons [26,27] and polaritons, where BEC is obtained in the lowest momentum state by collisions of higher states in the lower polariton branch [28]. As with polaritons, it is likely that spin-exchange interactions are increased by Bose stimulation due to the preexisting $m_s = -3$ condensate.

To produce multicomponent condensates during evaporation, we performed a second series of shock cooling experiments, with a lower magnetization $M = -2.00 \pm 0.25$ (where the uncertainty is associated with detection noise). The initial $m_s = -3$ thermal gas is now depolarized using a radio-frequency pulse. After decoherence of the spin components, this leads to a thermal incoherent mixture with an initial fractional population in the $m_s = -3, -2, -1,$ and 0 states of approximately 31%, 40%, 21%, and 6%, with a relative uncertainty of 10%. When shock cooling is performed fast ($t_S \approx 50$ ms), we observe the production of very small multicomponent condensates in all three of the lowest energy states (as illustrated in Figs. 1 and 4). Our numerical simulations show that spin dynamics has, again, a very profound influence on the dynamics of condensation. In practice, spin-excited states with $m_s > 0$ are not saturated. Therefore, spin dynamics tends to populate these nonsaturated states and empty the condensates, which thus remain small and short lived.

An important observation is that the spin distribution of the obtained multicomponent BECs shows strong fluctuations [see Fig. 4(a)] compared to the thermal fraction. We interpret this feature in the following way. Bose condensation of the different spin-excited states introduces a spontaneous symmetry breaking, as the phase of each condensate is chosen randomly. This spontaneous symmetry breaking, previously observed in Ref. [26], can also be interpreted as the production of fragmented BECs

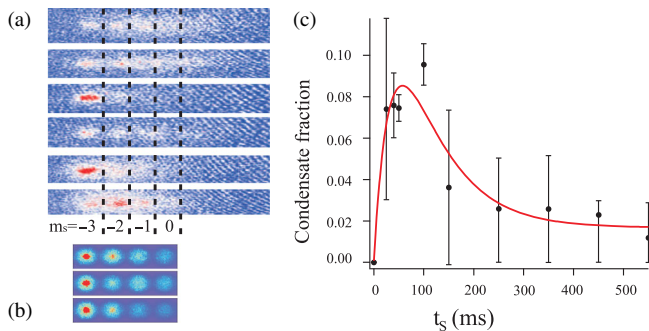


FIG. 4. (a) Absorption images after shock cooling experiments performed with $t_S = 50$ ms and an initial magnetization $M = -2 \pm 0.25$. A small BEC is present in the three lowest spin states; i.e., $m_s = -3, -2,$ and -1 . The different images illustrate the fluctuations of magnetization of the condensate fraction. (b) Numerical results after evaporation, for three initial relative sets of phases. (c) Total condensate fraction of the multispin component gas for $t = t_S$ and $M = -2 \pm 0.25$ as a function of t_S . We observe small multicomponent condensates in the three lowest energy states. The solid line is a guide for the eye.

[29,30]. As spin dynamics is sensitive to the relative phase between the condensates in the various spin states [9,31], we propose that the observed spin fluctuations result from the combined effect of spin dynamics and the spontaneous symmetry breaking.

We performed numerical simulations to test this scenario. As the CFA does not provide a direct way to provide symmetry breaking at the BEC transition, we chose to apply random relative phases to the wave functions, describing the thermal atoms in different spin components before condensation. This provides an empirical way to simulate symmetry breaking. We performed a series of numerical simulations for different sets of relative phases between the Zeeman components. We then obtained small condensates with fluctuating magnetization [see Fig. 4(b)]. Furthermore, we also observe that spin and condensation dynamics is also significantly modified by the applied random phases. Owing to the large computational time for each run, a systematic study of BEC magnetization as a function of the initial phases has not yet been performed and remains to be thoroughly investigated. However, while the magnetization fluctuations obtained in the numerical simulations are typically 3 times smaller than the experimental measurements, these preliminary results thus support the scenario that the combined effect of spontaneous symmetry breaking and spin dynamics leads to the observed spin fluctuations.

To conclude, our study reveals a strong interplay between Bose condensation and spin dynamics, which is of particular relevance when spin-dependent and spin-independent interactions take place on a similar time scale (in contrast to previous studies with alkali atoms; see Refs. [32,33]). This interplay can result in a delay in obtaining a BEC in spin-excited states or, alternatively, to the production of metastable spinor gases which decay due to spin-exchange collisions. Our results also show that the difficulty in fully thermalizing the spin degrees of freedom is a prominent effect to be taken into account for very large spin systems (such as Dy [15] and Er [14]), where all of the spin states must be saturated for a stable multicomponent BEC to be produced. Finally, we point out that when a multicomponent BEC is dynamically produced, spontaneous symmetry breaking, leading to independent phases within the BEC components, may explain the observed spin fluctuations.

This work was supported by Conseil Régional d'Ile de France through Domaine d'intérêt majeur NanoK- Institut Francilien de Recherche sur les atomes froids (IFRAF), Centre National de la Recherche scientifique (CNRS), Ministère de l'Enseignement Supérieur et de la Recherche within Contrat de Plan Etat Région (CPER), Université Sorbonne Paris Cité (USPC), and the Indo-French Centre for the Promotion of Advanced Research (CEFIPRA). M. B. and M. G. acknowledge support from National Science Center (Poland) Grant No. DEC-2012/04/A/ST2/00090.

- [1] A. M. Kaufman, M. Eric Tai, A. Lukin, M. Rispoli, R. Schittko, P. M. Preiss, and M. Greiner, *Science* **353**, 794 (2016).
- [2] M. Gring, M. Kuhnert, T. Langen, T. Kitagawa, B. Rauer, M. Schreitl, I. Mazets, D. A. Smith, E. Demler, and J. Schmiedmayer, *Science* **337**, 1318 (2012).
- [3] J.-y. Choi, S. Hild, J. Zeiher, P. Schauß, A. Rubio-Abadal, T. Yefsah, V. Khemani, D. A. Huse, I. Bloch, and C. Gross, *Science* **352**, 1547 (2016).
- [4] I. Shvarchuck, Ch. Buggle, D. S. Petrov, K. Dieckmann, M. Zielonkowski, M. Kemmann, T. G. Tiecke, W. von Klitzing, G. V. Shlyapnikov, and J. T. M. Walraven, *Phys. Rev. Lett.* **89**, 270404 (2002).
- [5] H.-J. Miesner *et al.*, *Science* **279**, 1005 (1998).
- [6] N. Navon, A. L. Gaunt, R. P. Smith, and Z. Hadzibabic, *Science* **347**, 167 (2015).
- [7] L. Chomaz, L. Corman, T. Bienaimé, R. Desbuquois, C. Weitenberg, S. Nascimbène, J. Beugnon, and J. Dalibard, *Nat. Commun.* **6**, 6162 (2015).
- [8] T.-L. Ho, *Phys. Rev. Lett.* **81**, 742 (1998); T. Ohmi and K. Machida, *J. Phys. Soc. Jpn.* **67**, 1822 (1998); D. M. Stamper-Kurn and M. Ueda, *Rev. Mod. Phys.* **85**, 1191 (2013).
- [9] Y. Kawaguchi and M. Ueda, *Phys. Rep.* **520**, 253 (2012).
- [10] P. Coleman, *Introduction to Many-Body Physics* (Cambridge University Press, Cambridge, England, 2016); M. Lewenstein, A. Sanpera, and V. Ahufinger, *Ultracold Atoms in Optical Lattices* (Oxford University Press, New York, 2012).
- [11] S. S. Natu and E. J. Mueller, *Phys. Rev. A* **84**, 053625 (2011).
- [12] A. Griesmaier, J. Werner, S. Hensler, J. Stuhler, and T. Pfau, *Phys. Rev. Lett.* **94**, 160401 (2005).
- [13] Q. Beaufils, R. Chicireanu, T. Zanon, B. Laburthe-Tolra, E. Maréchal, L. Vernac, J.-C. Keller, and O. Gorceix, *Phys. Rev. A* **77**, 061601(R) (2008); B. Naylor, A. Reigie, E. Maréchal, O. Gorceix, B. Laburthe-Tolra, and L. Vernac, *Phys. Rev. A* **91**, 011603(R) (2015).
- [14] K. Aikawa, A. Frisch, M. Mark, S. Baier, A. Rietzler, R. Grimm, and F. Ferlaino, *Phys. Rev. Lett.* **108**, 210401 (2012); K. Aikawa, A. Frisch, M. Mark, S. Baier, R. Grimm, and F. Ferlaino, *Phys. Rev. Lett.* **112**, 010404 (2014).
- [15] M. Lu, N. Q. Burdick, S. Ho Youn, and B. L. Lev, *Phys. Rev. Lett.* **107**, 190401 (2011); M. Lu, N. Q. Burdick, and B. L. Lev, *Phys. Rev. Lett.* **108**, 215301 (2012).
- [16] B. Pasquiou, G. Bismut, Q. Beaufils, A. Crubellier, E. Maréchal, P. Pedri, L. Vernac, O. Gorceix, and B. Laburthe-Tolra, *Phys. Rev. A* **81**, 042716 (2010).
- [17] N. Tammuz, R. P. Smith, R. L. D. Campbell, S. Beattie, S. Moulder, J. Dalibard, and Z. Hadzibabic, *Phys. Rev. Lett.* **106**, 230401 (2011).
- [18] K. Góral, M. Gajda, and K. Rzążewski, *Opt. Express* **8**, 92 (2001).
- [19] B. Pasquiou, E. Maréchal, L. Vernac, O. Gorceix, and B. Laburthe-Tolra, *Phys. Rev. Lett.* **108**, 045307 (2012).
- [20] M. Fattori, T. Koch, S. Goetz, A. Griesmaier, S. Hensler, J. Stuhler, and T. Pfau, *Nat. Phys.* **2**, 765 (2006).
- [21] B. Naylor, E. Maréchal, J. Huckans, O. Gorceix, P. Pedri, L. Vernac, and B. Laburthe-Tolra, *Phys. Rev. Lett.* **115**, 243002 (2015).
- [22] U. Ebling, J. S. Krauser, N. Flschner, K. Sengstock, C. Becker, M. Lewenstein, and A. Eckardt, *Phys. Rev. X* **4**, 021011 (2014).
- [23] M. Brewczyk, M. Gajda, and K. Rzążewski, *J. Phys. B* **40**, R1 (2007).
- [24] T. Karpiuk, M. Brewczyk, M. Gajda, and K. Rzążewski, *Phys. Rev. A* **81**, 013629 (2010).
- [25] T. Isoshima, T. Ohmi, and K. Machida, *J. Phys. Soc. Jpn.* **69**, 3864 (2000).
- [26] F. Fang, R. Olf, S. Wu, H. Kadau, and D. M. Stamper-Kurn, *Phys. Rev. Lett.* **116**, 095301 (2016).
- [27] S. O. Demokritov, V. E. Demidov, O. Dzyapko, G. A. Melkov, A. A. Serga, B. Hillebrands, and A. N. Slavin, *Nature (London)* **443**, 430 (2006).
- [28] J. Kasprzak, M. Richard, S. Kundermann, A. Baas, P. Jeambrun, J. M. J. Keeling, F. M. Marchetti, M. H. Szyman Acuteska, R. André, J. L. Staehli, V. Savona, P. B. Littlewood, B. Deveaud, and L. Si Dang, *Nature (London)* **443**, 409 (2006).
- [29] C. K. Law, H. Pu, and N. P. Bigelow, *Phys. Rev. Lett.* **81**, 5257 (1998); T.-L. Ho and S. Kit Yip, *Phys. Rev. Lett.* **84**, 4031 (2000).
- [30] L. De Sarlo, L. Shao, V. Corre, T. Zibold, D. Jacob, J. Dalibard, and F. Gerbier, *New J. Phys.* **15**, 113039 (2013).
- [31] M. S. Chang, Q. Qin, W. Zhang, L. You, and M. S. Chapman, *Nat. Phys.* **1**, 111 (2005).
- [32] H. Schmaljohann, M. Erhard, J. Kronjger, K. Sengstock, and K. Bongs, *Appl. Phys. B* **79**, 1001 (2004).
- [33] J. Guzman, G.-B. Jo, A. N. Wenz, K. W. Murch, C. K. Thomas, and D. M. Stamper-Kurn, *Phys. Rev. A* **84**, 063625 (2011).